The Variation of the Plasma Sheet Polytropic Index Along the Midnight Meridian in a Finite Width Magnetotail

AD-A225 948

H. E. SPENCE
Space Sciences Laboratory
Laboratory Operations
The Aerospace Corporation
El Segundo, CA 90245

and

M. G. KIVELSON
Department of Earth and Space Sciences and
Institute of Geophysics and Planetary Physics
University of California
Los Angeles, CA 90024

15 August 1990

Prepared for

SPACE SYSTEMS DIVISION
AIR FORCE SYSTEMS COMMAND
Los Angeles Air Force Base
P.O. Box 92960
Los Angeles, CA 90009-2960

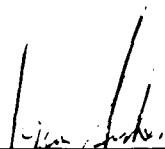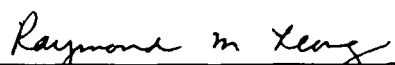This report was submitted by The Aerospace Corporation, El Segundo, CA 90245, under Contract No. F04701-88-C-0089 with the Space Systems Division, P.O. Box 92960, Los Angeles, CA 90009-2960. It was reviewed and approved for The Aerospace Corporation by H. R. Rugge, Acting Director, Space Sciences Laboratory.

Lt Fisher was the project officer for the Mission-Oriented Investigation and Experimentation (MOIE) Program.

This report has been reviewed by the Public Affairs Office (PAS) and is releasable to the National Technical Information Service (NTIS). At NTIS, it will be available to the general public, including foreign nationals.

This technical report has been reviewed and is approved for publication. Publication of this report does not constitute Air Force approval of the report's findings or conclusions. It is published only for the exchange and stimulation of ideas.

TYRON FISHER, LT, USAF
MOIE Project Officer
SSD/CLPO

RAYMOND M. LEONG, MAJ, USAF
MOIE Program Manager
AFSTC/WCO OL-AB

REPORT DOCUMENTATION PAGE

1a. REPORT SECURITY CLASSIFICATION Unclassified		1b. RESTRICTIVE MARKINGS
2a. SECURITY CLASSIFICATION AUTHORITY		3. DISTRIBUTION/AVAILABILITY OF REPORT Approved for public release; distribution unlimited
2b. DECLASSIFICATION/DOWNGRADING SCHEDULE		
4. PERFORMING ORGANIZATION REPORT NUMBER(S) TR-0089(4940-06)-8		5. MONITORING ORGANIZATION REPORT NUMBER(S) SSD-TR-90-17
6a. NAME OF PERFORMING ORGANIZATION The Aerospace Corporation Laboratory Operations	6b. OFFICE SYMBOL (If applicable)	7a. NAME OF MONITORING ORGANIZATION Space Systems Division
6c. ADDRESS (City, State, and ZIP Code) El Segundo, CA 90245-4691		7b. ADDRESS (City, State, and ZIP Code) Los Angeles Air Force Base Los Angeles, CA 90009-2960
8a. NAME OF FUNDING/SPONSORING ORGANIZATION	8b. OFFICE SYMBOL (If applicable)	9. PROCUREMENT INSTRUMENT IDENTIFICATION NUMBER F04701-88-C-0089
8c. ADDRESS (City, State, and ZIP Code)		10. SOURCE OF FUNDING NUMBERS

10. SOURCE OF FUNDING NUMBERS			
PROGRAM ELEMENT NO.	PROJECT NO.	TASK NO.	WORK UNIT ACCESSION NO.

11. TITLE (Include Security Classification)

The Variation of the Plasma Sheet Polytropic Index Along the Midnight Meridian in a Finite Width Magnetotail

12. PERSONAL AUTHOR(S)

Spence, H. E., and Kivelson, M. G.

13a. TYPE OF REPORT	13b. TIME COVERED FROM _____ TO _____	14. DATE OF REPORT (Year, Month, Day) 15 August 1990	15. PAGE COUNT 14

16. SUPPLEMENTARY NOTATION

17. COSATI CODES			18. SUBJECT TERMS (Continue on reverse if necessary and identify by block number)
FIELD	GROUP	SUB-GROUP	Magnetospheric Configuration Magnetotail Plasma Convection Plasma Sheet

19. ABSTRACT (Continue on reverse if necessary and identify by block number)

We have obtained the polytropic index as a function of distance along the midnight meridian in the terrestrial magnetotail. As our purpose is to establish the effects of the finite width of the magnetotail, we use a simple theoretical model of plasma sheet convection, i.e., two-dimensional field structure and adiabatic inward convection of a uniform distant tail source. Particle orbits are treated independently for portions of the phase space distribution on shells of constant energy. On the midnight meridian, the moments of the distribution are parameterized by τ, the ratio of half the cross-tail potential energy to the characteristic Maxwellian energy of a distant down-tail plasma source. We infer from the model the plasma pressure, P, and the number density, n, along the midnight meridian as a function of τ. P and n define locally an "effective" polytropic index, γ. We find that γ ranges between 5/3 and 1, depending on the value of τ and on geocentric distance. We suggest that the qualitative differences between the recent empirical determinations of the polytropic index by Baumjohann and Paschmann and Huang et al. may be accounted for in part by this simple model.

20. DISTRIBUTION/AVAILABILITY OF ABSTRACT ☐ UNCLASSIFIED/UNLIMITED ☒ SAME AS RPT. ☐ DTIC USERS	21. ABSTRACT SECURITY CLASSIFICATION Unclassified	
22a. NAME OF RESPONSIBLE INDIVIDUAL	22b. TELEPHONE (Include Area Code)	22c. OFFICE SYMBOL

DD FORM 1473, 84 MAR   83 APR edition may be used until exhausted.
All other editions are obsolete   SECURITY CLASSIFICATION OF THIS PAGE

UNCLASSIFIED

CONTENTS

FIGURES

A-1

I. INTRODUCTION

An important relationship used commonly in magnetohydrodynamic (MHD) descriptions of convection in the earth's plasma sheet is one that links plasma pressure, P, and mass density, ρ. The equation of state, $P = \alpha\rho^{5/3}$, where α is a constant of motion, emerges from the combined MHD mass, momentum, and energy equations if a scalar pressure and an adiabatic (constant entropy) flow are assumed (see *Siscoe* [1983]). For more general conditions, the equation of state can be used in its polytropic form, $P = \alpha\rho^{\gamma}$, where γ is the polytropic index.

We address, in this report, the "effective" polytropic equation of state in the earth's magnetotail by developing further a theoretical model of plasma sheet convection. The model extends the analysis of *Kivelson and Spence* [1988], who showed that during sufficiently slow earthward convection, a flux tube's integrity is violated because cross-tail (gradient/curvature) drift of the energetic particle population is large, relative to the bulk earthward ($\mathbf{E} \times \mathbf{B}$) drift. [This effect can be incorporated as a cross-tail heat flux in an MHD description (Goertz, personal communication, 1989).] Consequently, pressures calculated in a magnetotail of finite width can be reduced significantly from those calculated using two-dimensional (2D), lossless adiabatic convection models. In this report, we determine the effect of the finite tail width on number density and find that flux-tube content is not a constant of motion along the midnight meridian. Finally, we use the modeled pressures and number densities to define an effective polytropic equation of state.

II. CONVECTION MODEL

We adopt the modified model of plasma sheet convection presented first by *Erickson* [1985] and discussed more recently by *Kivelson and Spence* [1988]. We assume for simplicity a zero dipole tilt and use geocentric solar magnetospheric (GSM) coordinates. At a large down-tail distance X_0 (taken to be -60 R_E), we assume that a uniform plasma, characterized by a Maxwellian temperature, T_0, and a number density, n_0, is the source of plasma for the tail plasma sheet. The plasma is distributed uniformly across a tail of width $2R$. In this treatment, we do not include low latitude boundary layer (LLBL) particles that drift in from the dawn magnetopause. The LLBL constitutes a source of additional particles for the near-earth plasma sheet, so by ignoring it, we underestimate the density and pressure along the midnight meridian. We assume that earthward convection of the plasma is driven by a uniform magnetotail electric field, E, pointing from dawn to dusk and that the 2D magnetic field is given by the midnight meridian cut through the $Kp = 0, 0^+$ *Tsyganenko* [1987] (T87) model (see his Figure 2). Hence the model is pertinent to the magnetotail under geomagnetically quiescent conditions. Furthermore, we assume that pitch angle scattering maintains isotropic distributions upon convection. We describe the motion of the bounce orbit at the equatorial (X-Y) plane at $Z = 0$ using bounce-averaged drift theory. At a location earthward of the source, $(X_e,0,0)$, the spectrum of particles arriving from the source cuts off above a critical energy which, by conservation of energy, can be related to a critical energy, $W_0{}^m$, in the source spectrum. The value of $W_0{}^m$ depends on the parameters of the convection process as $W_0{}^m = qER/\left([V_0/V(X_e)]^{\frac{2}{3}} - 1\right)$, where $V(X_e)$ [V_0] is the specific volume of the flux tube intersecting X_e [X_0] [*Kivelson and Spence*, 1988]. Particles starting from $(X_0,Y,0)$ with $W_0 > W_0^m$ acquire cross-tail velocities that sweep them duskward of midnight before they reach X_e.

Macroscopic plasma parameters are obtained from velocity moments of the distribution function, and Liouville's theorem specifies the mapping of phase space density from X_0 to X_e. The upper bound to the velocity integrals that yield the desired moments is defined by $W_0{}^m$ [$v_0{}^m = (2W_0{}^m/m_p)^{\frac{1}{2}}$] and is finite if $R < \infty$. Note that we assume protons, with mass, m_p, dominate the plasma sheet plasma, and we neglect electrons and heavy ions. *Erickson* [1985] and *Kivelson and Spence* [1988] showed that the plasma pressure at X_e in a finite width tail is reduced, relative to that in an infinitely wide (2D) tail, by the fraction

$$\frac{P_R(X_e)}{P_\infty(X_e)} = erf(\zeta) - 2\zeta(3 + 2\zeta^2)exp(-\zeta^2)/3(\pi)^{\frac{1}{2}} \tag{1}$$

where $erf(\zeta)$ is the error function and

$$\zeta^2 = W_0{}^m/kT_0 = \tau/\left([V_0/V(X_e)]^{\frac{2}{3}} - 1\right) \tag{2}$$

$$\tau = qER/kT_0 \tag{3}$$

P_∞ was obtained from the relation $P_\infty \propto V^{-\gamma}$, where the polytropic index, γ, was taken to be $\frac{5}{3}$. *Kivelson and Spence* [1988] evaluated Eq. (1) and showed that for low values of τ ($\tau < 10$), the finite tail width effect can lead to pressure ratios significantly less than 1 and

5

may provide a resolution to the "pressure-balance inconsistency" described by *Erickson and Wolf* [1980].

We next consider the degree to which number density profiles are modified by the finite tail width effect. For the case of 2D, lossless convection, flux-tube content is a constant of motion, and this requirement specifies the radial variation of n according to $nV = constant$. We next determine the variation of n in a finite width tail by calculating the zeroth velocity moment of the distribution function whose second moment yielded Eq. (1). Here we assume that protons are the dominant ion species, and we relate the mass density to the ion number density by $\rho_m = nm_p$. We find that the ratio of the number density in a tail of finite width relative to that in an infinitely wide tail ($n_\infty = n_0 V_0/V$) is given by

$$\frac{n_R(X_e)}{n_\infty(X_e)} = erf(\zeta) - 2\zeta exp(-\zeta^2)/\pi^{\frac{1}{2}} \tag{4}$$

In Figure 1, we have plotted the number density ratio, n_R/n_∞, versus the flux-tube volume ratio, V_0/V, as a function of τ. As τ approaches infinity (i.e., a 2D magnetotail), $n_R \approx n_\infty$. The departure of the number density from that predicted by constant flux-tube content is less than 10% for $\tau > 50$ (see topmost curve in Figure 1) and is only weakly dependent on the compression ratio, V_0/V. On the other hand, as τ decreases to small values, n_R/n_∞ becomes significantly less than 1 for sufficiently large compression. For $\tau = 10$, n_R is approximately 0.4 (0.6, 0.8) the value predicted by the requirement of constant flux-tube volume for a compression ratio of 45 (17, 10).

To show more clearly how flux-tube content changes with inward convection, we have plotted nV versus X_e in Figure 2a. The flux-tube volume (obtained from the T87 model) and the number density have been normalized by their values at 60 R_E: $V_0 = 7.5 \times 10^{16}$ m^3/Wb and $n_0 = 0.1$ cm^{-3} (consistent with the quiet time values observed near lunar orbit by *Rich et al.* [1973]). Figure 2a shows that nV is nearly constant beyond ~ 30 R_E for all interesting values of τ. At these distances, the finite tail width effect is unimportant. At radial distances less than 30 R_E, the normalized flux-tube content drops noticeably below 1 at a location that shifts earthward with increasing τ. For example, for $\tau < 10$, $nV = constant$ overestimates the density in the near-magnetotail by a factor ≥ 3.

In Figure 2b we have plotted n_R versus distance along the midnight meridian as given by Eq. (4). Curves are parameterized by τ and are normalized to 0.1 cm^{-3} at 60 R_E. As noted in Figure 2a, the finite tail width has little effect on the radial profile of number density beyond 30 R_E; however, the dependence of n_R on τ is strong for $X_e < 20$ R_E. We know that the quiet time central plasma sheet number density rarely exceeds 1 cm^{-3} between 10 and ~ 20 R_E [*Baumjohann and Paschmann*, 1989; *Huang et al.*, 1989]. This empirical constraint, when combined with the curves in Figure 2b, argues for $\tau \leq 7$ during quiet times. We note that $\tau \leq 7$ is consistent with the value determined by *Kivelson and Spence* [1988], who found that $\tau \leq 5$ was required for the modeled pressure profile in the near-earth plasma sheet not to exceed the lobe magnetic pressure. These limits on τ may require modification when the LLBL source of plasma is included in the model.

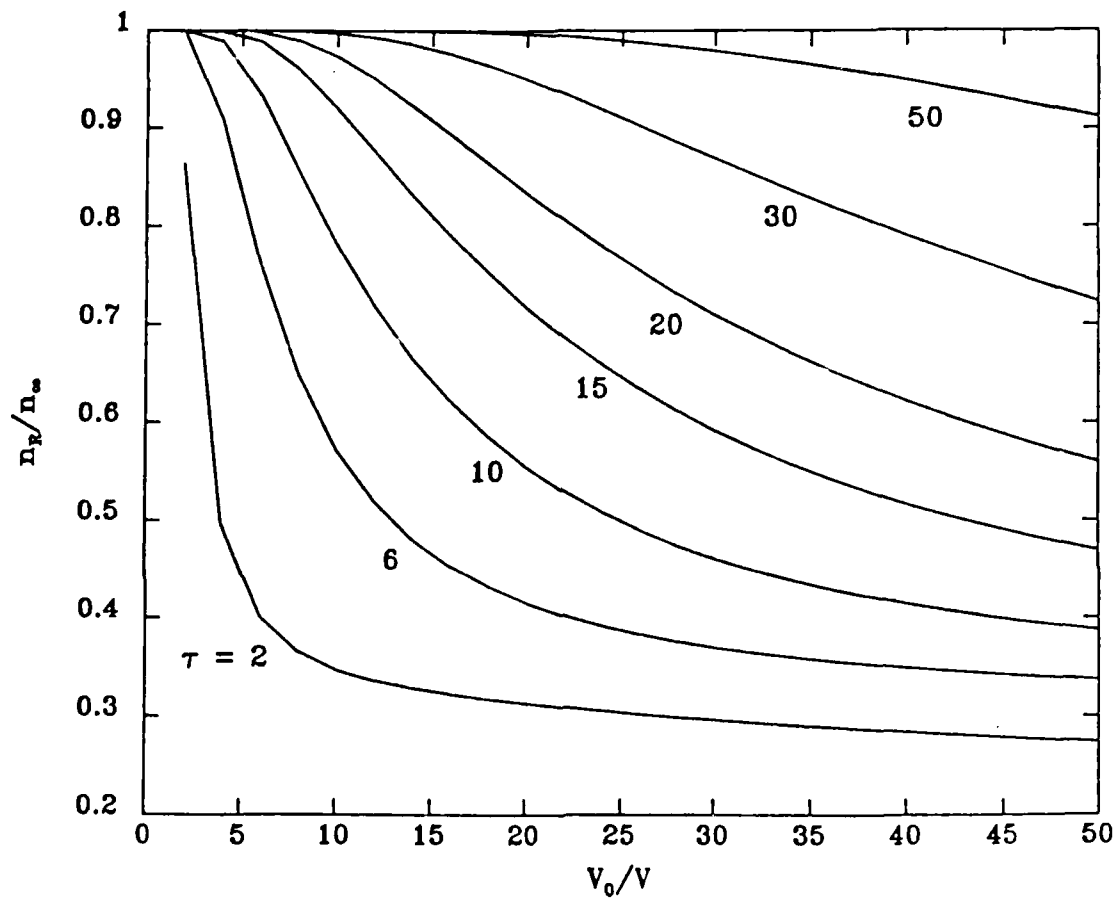Figure 1. The ratio (n_R/n_∞) of the number density along the midnight meridian in a tail of width $2R$ to the number density in a tail of infinite width versus the ratio (V_0/V) of the flux-tube volumes at the source location and closer to the earth. The curves are labeled τ, the ratio of the potential drop across half of the tail to the thermal energy per unit charge in the source distribution.
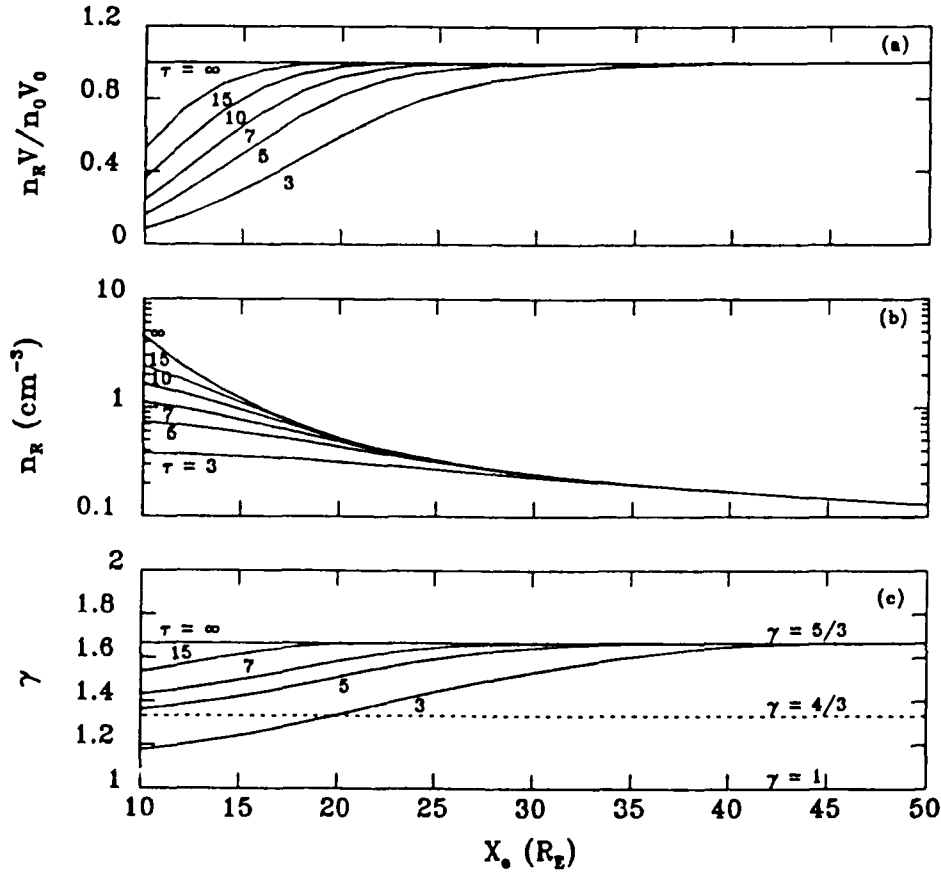
Figure 2. Normalized flux-tube content (a), number density (b), and the "effective" locally determined polytropic index (c) plotted versus distance in the magnetic equatorial plane along the midnight meridian as a function of τ. In a, nV is normalized by its value at 60 R_E. In b, the n_∞ curve is obtained by the assumption of lossless convection in a tail of infinite width (i.e., $nV = constant$). In c, for large values of τ and/or large down-tail distances, γ is nearly $\frac{5}{3}$; for $\tau < 15$ and for relatively small down-tail distances, γ may take on values much less than $\frac{5}{3}$.

III. DETERMINATION OF THE RADIAL VARIATION OF THE POLYTROPIC INDEX

In this section, we use the modeled pressure and number density to define locally a polytropic index, γ, where $P/P_0 = (n/n_0)^\gamma$. For an infinitely wide magnetotail, $\tau = \infty$ and $\gamma = \frac{5}{3}$. Results for other values of τ are shown in Figure 3, where we have plotted n_R/n_0 versus P_R/P_0 on logarithmic scales. All curves were normalized to a pressure and density at X_0 consistent with observations. For an assumed polytropic relation between P_R/P_0 and n_R/n_0, the slopes of the curves in Figure 3 determine local values of γ (dashed lines identify slopes corresponding to $\gamma = \frac{5}{3}$ and 1). The slope of the topmost solid curve ($\tau = \infty$) is $\frac{5}{3}$, corresponding to adiabatic convection in the 2D fluid limit. Note that as τ decreases, the slopes of the curves become shallower as the density increases. This indicates that flux tubes close to the inner edge of the tail which are greatly compressed have local values of $\gamma < \frac{5}{3}$.

Using the slopes of the curves in Figure 3, we have obtained values of the locally defined γ as a function of distance, and we show the results for different values of τ in Figure 2c. Dashed horizontal lines identify $\gamma = \frac{5}{3}$, $\frac{4}{3}$, and 1. For $X_e > 40\ R_E$, $\gamma \sim \frac{5}{3}$ for all values of τ that we consider. At these large down-tail distances, the finite tail corrections to P and n are relatively unimportant, because cross-tail drifts are small compared to sunward $\mathbf{E} \times \mathbf{B}$ drifts and the integrity of plasma within a flux tube is effectively maintained upon convection. However, for $X_e < 40\ R_E$, γ is sensitive to both X_e and τ. For small values of τ, γ departs from the $\tau = \infty$ curve. The location where γ deviates significantly from $\frac{5}{3}$ moves down tail (larger X_e) with decreasing τ. We note that for nominal τ (≤ 7), our model predicts $\gamma \leq \frac{4}{3}$ at $X_e \sim 10\ R_E$ and $1 \leq \gamma \leq \frac{5}{3}$ at $X_e \sim 20\ R_E$.

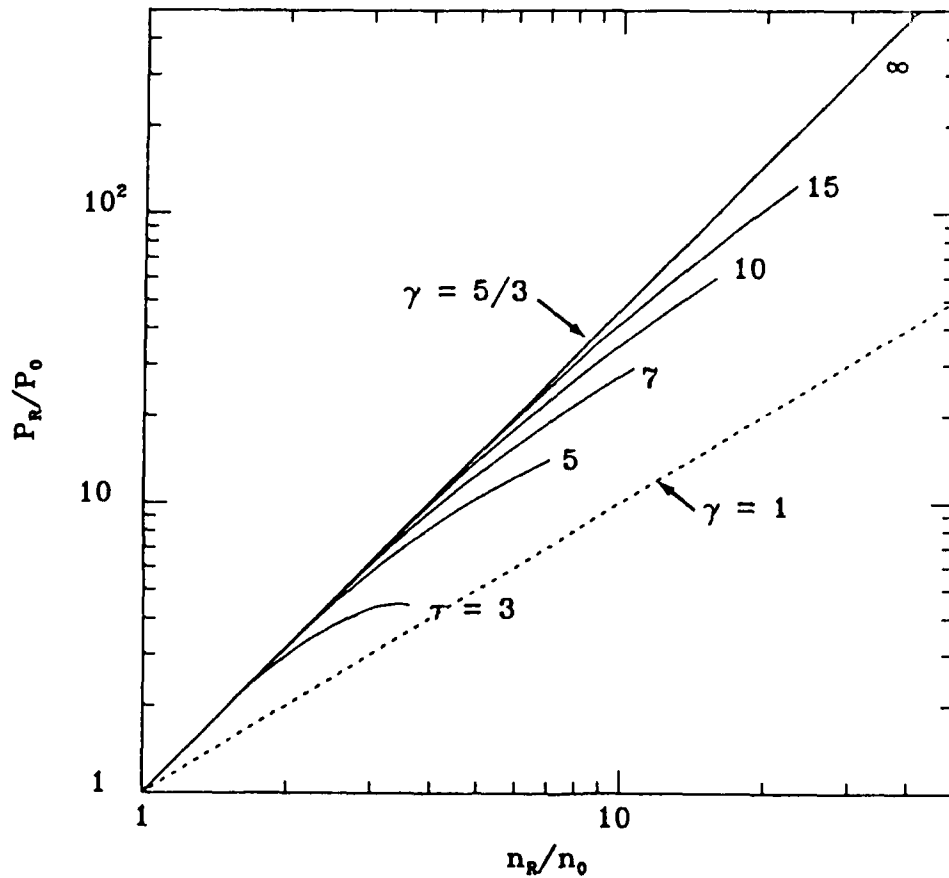Figure 3. Solid curves show the relationship between P_R/P_0 and n_R/n_0 on a logarithmic scale as a function of τ. The curves' slopes define locally a polytropic index, γ; the dashed lines indicate γ's of $\frac{5}{3}$ and 1. As τ approaches infinity, γ approaches $\frac{5}{3}$; for smaller values of τ, slopes are shallower and, therefore, $\gamma < \frac{5}{3}$.

IV. QUALITATIVE COMPARISON OF γ WITH *IN SITU* DETERMINATIONS

Recently, two independent data surveys determined γ empirically in the quiet-time, near-tail plasma sheet. *Baumjohann and Paschmann* [1989] analyzed an extensive data set comprised of plasma pressure and density moments obtained at 4.5 s resolution with the ion release module (IRM) three-dimensional (3D) plasma instrument. Data were obtained when the IRM spacecraft was in the geomagnetic tail ($-9 \geq X_{GSM} \geq -19$, $|Y_{GSM}| \leq 12$, $2 \leq Z_{NS} \leq -9$), and individual measurements were identified as being either from the central plasma sheet (CPS) or from the plasma sheet boundary layer (PSBL).

Baumjohann and Paschmann [1989] plotted log pressure versus log density (both CPS and PSBL) in the same format as our Figure 3 and performed linear regression analysis on the data. They found that the best-fit slope implied $\gamma = 1.69$. They also investigated γ in the CPS and the PSBL separately and found that, while P and n were well correlated and $\gamma = 1.59$ in the PSBL, the correlation was too low to determine a meaningful index in the CPS. Despite the simplicity of our model, we believe these results are qualitatively consistent with its predictions. Measurements obtained in the PSBL (i.e., at higher magnetic latitudes, where the vertical distance from the neutral sheet is relatively large) will normally map to equatorial locations well down tail from IRM's X_{GSM} location. Finite tail width effects are relatively small at these distances and, therefore, we predict that γ will differ little from $\frac{5}{3}$. On the other hand, measurements obtained in the CPS are presumably taken much closer to the magnetic equator and therefore map to equatorial locations in the near-vicinity of the IRM orbit. At these distances, our model predicts γ's ranging from 1 to $\frac{5}{3}$, with values highly dependent on both location and τ. Consequently, a poor correlation between CPS P and n is expected in a statistical sample that has not been binned according to location and geomagnetic activity. Finally, *Baumjohann and Paschmann* [1989] binned the combined CPS and PSBL data into two auroral electrojet (AE) index bins ($\lesssim 100$ nT) and found $\gamma \sim \frac{5}{3}$ for the active subset and $\sim \frac{4}{3}$ for the geomagnetically quieter subset. If larger E and τ correspond to higher levels of AE, these results are qualitatively consistent with the model predictions and are also quantitatively plausible. Binning of the data by location and activity would provide additional tests of this model and forthcoming modifications of it that will include LLBL plasma sources.

Huang et al. [1989] also determined γ empirically in the magnetotail plasma sheet. Their survey is comprised of plasma density and temperature ($kT = P/n$) estimates obtained by the low energy proton and electron differential energy analyzers (LEPEDEA) instrument on the international sun-earth explorer-1 (ISEE-1) spacecraft. The Huang et al. study concentrated on measurements from geomagnetically quiet intervals ($AE < 100$ nT) when ISEE-1 was in the CPS (between $-10 \leq X_{GSM} \leq -23\ R_E$). Log temperature was plotted versus log number density, and the slope of the best-fit linear trend was used to determine γ. Even though the correlation coefficient between temperature and density is relatively low, Huang et al. concluded that the two quantities are anticorrelated and therefore that $\gamma < 1$. In our model, we find that γ can be significantly $< \frac{5}{3}$ in the slowly convecting near-tail CPS but that it is everywhere ≥ 1. Elsewhere (*Spence and Kivelson*, in preparation, 1990), we will show that even for a locally defined $\gamma > 1$, the temperature can increase with distance in regions where the density is decreasing with distance.

V. SUMMARY

We have developed a theoretical model of plasma sheet convection for a plasma source in the distant tail to determine how number density varies with down-tail distance near the midnight meridian. We find that flux-tube content is not conserved during periods of slow convection. This means that an MHD formulation of the convection problem may have to include not only the previously noted cross-tail heat flux but also a cross-tail mass flux. Modeled number densities were combined with previously modeled pressures to construct locally a polytropic index. We find that γ ranges between 1 and $\frac{5}{3}$. Low values of γ occur during periods of small τ (intervals of slow convection) in the near-tail plasma sheet ($< 20\ R_E$), while values nearer $\frac{5}{3}$ occur during periods of larger τ (intervals of significantly enhanced convection) and/or at larger down-tail distances ($> 30\ R_E$). We feel that this model may in part explain some of the apparent discrepancy in the two empirical determinations [*Baumjohann and Paschmann*, 1989; *Huang et al.*, 1989] of the plasma sheet γ. Further meaningful comparison with data may require refinement of the model.

Possibly the most serious flaw in the present work is the neglect of an LLBL source. The contribution of such a source will be described elsewhere. Preliminary calculations show that the LLBL source modifies the solution along the midnight meridian by increasing n and P in regions where the pressure from the distant tail source drops below the lobe magnetic pressure. Including the LLBL source should reduce the pressure imbalance apparent in Figure 2 of *Kivelson and Spence* [1988] for small τ inside of 20 R_E. The LLBL source is also capable of partially populating the high-energy part of the distribution in the near-earth tail that is absent (because of the energy cutoff previously described) if only a tail source is considered.

Features of the model that require further examination include the variation of the moments with cross-tail distance and the effects of skewed or nonuniform electric fields [*Atkinson*, 1984] and of 3D magnetic structure. The consideration of y-dependence raises the question of electron reponse. The model implies a y-dependence of T_e/T_i in the near-earth plasma sheet, but no striking variation has been reported. Possibly the consideration of the field-aligned currents consistent with this model will eliminate this apparent discrepancy between model and data.

REFERENCES

Atkinson, G., Thick current sheets in the renovated model of the magnetosphere, *J. Geophys. Res.*, *89*, 8949, 1984.

Baumjohann, W., and G. Paschmann, Determination of the polytropic index in the plasma sheet, *Geophys. Res. Lett.*, *16*, 295, 1989.

Erickson, G. M., and R. A. Wolf, Is steady state convection possible in the earth's magnetosphere?, *Geophys. Res. Lett.*, *6*, 897, 1980.

Erickson, G. M., Modeling of plasma-sheet convection: Implications for substorms, Ph. D. dissertation, Rice Univ., Houston, TX, 1985.

Huang, C. Y., C. K. Goertz, L. A. Frank, and G. Rostoker, Observational determination of the adiabatic index in the quiet time plasma sheet, *Geophys. Res. Lett.*, *16*, 563, 1989.

Kivelson, M. G., and H. E. Spence, On the possibility of quasi-static convection in the quiet magnetotail, *Geophys. Res. Lett.*, *15*, 1541, 1988.

Rich, F. J., D. L. Reasoner, and W. J. Burke, Plasma-sheet at lunar distance: characteristics and interaction with the lunar surface, *J. Geophys. Res.*, *78*, 8097, 1973.

Siscoe, G. L., Solar system magnetohydrodynamics, in *Solar-Terrestrial Physics*, ed. by R. L. Carovillano and J. M. Forbes, pp. 11-100, Reidel, Dordrecht, 1983.

Tsyganenko, N. A., Global quantitative models of the geomagnetic field in the cislunar magnetosphere for different disturbance levels, *Planet. Space Sci.*, *35*, 1347, 1987.

LABORATORY OPERATIONS

The Aerospace Corporation functions as an "architect-engineer" for national security projects, specializing in advanced military space systems. Providing research support, the corporation's Laboratory Operations conducts experimental and theoretical investigations that focus on the application of scientific and technical advances to such systems. Vital to the success of these investigations is the technical staff's wide-ranging expertise and its ability to stay current with new developments. This expertise is enhanced by a research program aimed at dealing with the many problems associated with rapidly evolving space systems. Contributing their capabilities to the research effort are these individual laboratories:

Aerophysics Laboratory: Launch vehicle and reentry fluid mechanics, heat transfer and flight dynamics; chemical and electric propulsion, propellant chemistry, chemical dynamics, environmental chemistry, trace detection; spacecraft structural mechanics, contamination, thermal and structural control; high temperature thermomechanics, gas kinetics and radiation; cw and pulsed chemical and excimer laser development, including chemical kinetics, spectroscopy, optical resonators, beam control, atmospheric propagation, laser effects and countermeasures.

Chemistry and Physics Laboratory: Atmospheric chemical reactions, atmospheric optics, light scattering, state-specific chemical reactions and radiative signatures of missile plumes, sensor out-of-field-of-view rejection, applied laser spectroscopy, laser chemistry, laser optoelectronics, solar cell physics, battery electrochemistry, space vacuum and radiation effects on materials, lubrication and surface phenomena, thermionic emission, photosensitive materials and detectors, atomic frequency standards, and environmental chemistry.

Electronics Research Laboratory: Microelectronics, solid-state device physics, compound semiconductors, radiation hardening; electro-optics, quantum electronics, solid-state lasers, optical propagation and communications; microwave semiconductor devices, microwave/millimeter wave measurements, diagnostics and radiometry, microwave/millimeter wave thermionic devices; atomic time and frequency standards; antennas, rf systems, electromagnetic propagation phenomena, space communication systems.

Materials Sciences Laboratory: Development of new materials: metals, alloys, ceramics, polymers and their composites, and new forms of carbon; nondestructive evaluation, component failure analysis and reliability; fracture mechanics and stress corrosion; analysis and evaluation of materials at cryogenic and elevated temperatures as well as in space and enemy-induced environments.

Space Sciences Laboratory: Magnetospheric, auroral and cosmic ray physics, wave-particle interactions, magnetospheric plasma waves; atmospheric and ionospheric physics, density and composition of the upper atmosphere, remote sensing using atmospheric radiation; solar physics, infrared astronomy, infrared signature analysis; effects of solar activity, magnetic storms and nuclear explosions on the earth's atmosphere, ionosphere and magnetosphere; effects of electromagnetic and particulate radiations on space systems; space instrumentation.